PROCEEDINGS OF SPIE

MIPPR 2005

SAR and Multispectral Image Processing

Liangpei Zhang
Jianqing Zhang
Mingsheng Liao
Chairs/Editors

31 October–2 November 2005
Wuhan, China

Sponsored by
LIESMARS—State Key Laboratory of Information Engineering in Surveying, Mapping and Remote Sensing (China)
Wuhan University (China)

Cosponsored and Published by
SPIE—The International Society for Optical Engineering

Volume 6043
Part One of Two Parts

The International Society for Optical Engineering

Automatic extraction of tree rows and hedges by data integration techniques

Yongjun Zhang[a] Hongchao Bin[a, b]
School of Remote Sensing and Information Engineering, Wuhan University, 129 Luoyu Road, 430079, China
DongGuan Land and Resources Bureau, 268 East City Road, DongGuan, China
Email: zhangyj@whu.edu.cn, yongjun_zhang@hotmail.com

ABSTRACT

Data integration is a very important strategy to obtain optimum solutions in geo-scientific analysis, 3D scene modelling and visualization. This paper mainly focuses on the integration of GIS data, stereo aerial imagery and DSM to derive automatically tree rows and hedges in the open landscape. The roads, field boundaries, rivers and railways from GIS database also represent potential search areas for extracting tree rows and hedges, which are often located parallel and near to them. Different approaches, such as image segmentation by CIE L*a*b, edge extraction, linking, line grouping, space intersection and 3D verifying with DSM, are combined together to extract the objects of interest. The extracted information of tree rows and hedges can be used in many applications, such as deriving of wind erosion risk fields for soil monitoring and protection.

Keywords: Extraction, Integration, GIS, InfraRed, Image, Vegetation, Analysis, Segmentation

1. INTRODUCTION

Wind erosion causes loss of fertility, loss of organic matter, and reduce water holding capacity. It is a menace to the farmer and even to whole world (Driehuyzen M. G., 2003). Tree rows and hedges in the open landscape can decrease the speed of wind and thus protect the soil. So they are very important for soil monitoring and protection. Although considerable results have been achieved, the extraction of vegetation objects from high-resolution imagery is still not in an advanced period (Heipke et al. 2000, Straub 2003). To facilitate automated object extraction from aerial imagery, the use of prior knowledge is essential (Baltsavias 2002, Straub 2003). Prior work of extraction of tree rows and hedges in the open landscape is much more marginal. Intermediate results of extraction of tree rows and hedges are presented by Zhang (Zhang 2004) in XXth ISPRS Congress.

Digital color InfraRed (CIR) imagery is very important in data acquisition and updating, especially for vegetations. The Normalized Difference Vegetation Index (NDVI) is widely used in photogrammetry and remote sensing applications, such as monitoring of vegetation condition and production in change detection (Lyon et al 1998), extracting of trees in urban areas (Straub 2003) and relations between NDVI and tree productivity (Wang 2004). The CIE L*a*b color space is mainly used in computer vision communities for image analysis and industrial applications (Campadelli 2000, Lebrun 2000). However, it seems not of much interest by experts in photogrammetry and remote sensing despite its powerfulness in image segmentation and analysis.

This paper mainly focuses on automatic extraction of tree rows and hedges in the open landscape by data integration technique. Geographical Information System (GIS) data, Digital Surface Models (DSM) and CIR aerial stereo imagery are used as sources of information. General strategy and the data sources used for extraction of tree rows and hedges are described in the next section. Then the algorithms of image segmentation with CIE L*a*b is addressed. Afterwards, detailed workflow of how to extract tree rows and hedges, including image segmentation, line extraction and linking, line grouping and matching, verifying with DSM is presented. Results of automatically derived tree rows and hedges are given in section 5. Finally, discussions are given and further work is highlighted.

MIPPR 2005: SAR and Multispectral Image Processing, edited by Liangpei Zhang, Jianqing Zhang, Mingsheng Liao, Proc. of SPIE Vol. 6043, 60430Z, (2005) · 0277-786X/05/$15 · doi: 10.1117/12.654875

2. GENERAL STRATEGY AND DATA SOURCES

2.1 General strategy

The automatic extraction of tree rows and hedges by integrating GIS data, CIR stereo imagery as well as DSM is the purpose of the current research. The related work such as semantic modeling, extraction and updating of field boundaries (Butenuth et al 2003, Butenuth 2004) are not of interest in this paper, although tree rows and hedges are often field boundaries or at least can help to extract field boundaries. The non-vegetation areas in CIR images are removed by image segmentation with CIE L*a*b. Afterwards, edges of tree rows and hedges are extracted with Canny edge extraction algorithm followed by line linking, grouping and matching. Lines belong to non-interested regions such as urban, forests in the stereo imagery are masked out by GIS data. DSM is also considered in line grouping because of usually short distance and low contrast between adjacent hedge and tree row. Then the matched lines are projected onto the landscape with known camera parameters of the stereo images. Finally, height information provided by DSM is used to verify the potential tree rows and hedges since they are always higher than the landscape.

2.2 Test data sources

GIS data with accuracy of about 3m consists of the initial scene description. Since only tree rows and hedges are of interest, regions where no tree rows and hedges exist (e.g. urban, water, forest) in the imagery can be masked out by the available GIS data. Furthermore, the GIS objects road, river and railway represent potential search areas for tree rows and hedges, which are usually located parallel and near to them. Figure 1 shows the GIS data superimposed on the aerial image in the open landscape. Roads and field boundaries are depicted in yellow, buildings in white, and forests in green. A representative region of interest is highlighted in dashed white lines and shown in Figure 2 separately.

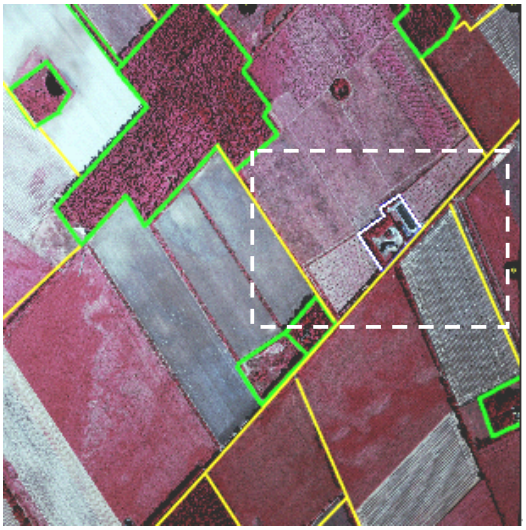

Figure 1. Open landscape with superimposed GIS data

CIR images with ground resolution of 0.5m are generated in early autumn when the vegetation is in an advanced period of growth. The color is almost fully green for tree rows and hedges, while for example light yellow for crops. The color information is of great advantageous for automatic extraction. Therefore, the color space RGB, which presents the raw stereo CIR images, is transformed into a device type independent color space CIE L*a*b since it is powerful in image segmentation. The CIR image is segmented into vegetation and non-vegetation regions. Of course, there are other objects than tree rows and hedges, which will appear in green color such as grassland. That means GIS data and CIR imagery are not enough to extract tree rows and hedges.

Additionally, corresponding DSM with 0.5 m ground resolution of the interested area is produced with VirtuoZo. As shown in Figure 3, the DSM is not precise because control points are obtained from the 3m resolution GIS data. But the field of interest in the open landscape is mostly flat, and tree rows and hedges are always higher. So height information from the DSM is still one of the useful sources of information, which can be integrated into a combined model together with GIS data and color information to support the extraction process.

Figure 2. Selected region of interest

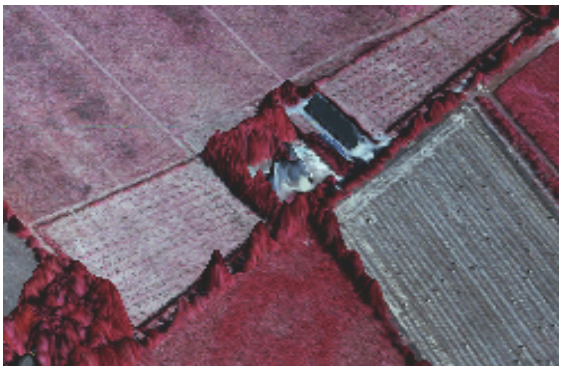

Figure 3. DSM superimposed with orthoimage

3. IMAGE SEGMENTATION BY CIE L*A*B

In 1931, Commission Internationale de l'Eclairage (CIE) presented a device independent color space CIE XYZ (SEII EM-MI 2002). Three axes X, Y, Z are orthogonally defined by the basic colors R, G, B. Generally, only points on surface $X+Y+Z=1$ are considered. This surface includes a white point (Wx, Wy, Wz) with value $(0.312779,\ 0.329184,\ 0.358037)$ and three settlements for the basic colors R, G, B.

Each point in color space RGB has its corresponding point in color space CIE XYZ. The linear model of transformation from RGB to CIE XYZ can be written as follows:

$$\begin{bmatrix} X \\ Y \\ Z \end{bmatrix} = \begin{bmatrix} 0.412291 & 0.357664 & 0.180209 \\ 0.212588 & 0.715329 & 0.072084 \\ 0.019326 & 0.119221 & 0.949102 \end{bmatrix} \cdot \begin{bmatrix} R \\ G \\ B \end{bmatrix} \tag{1}$$

The color space CIE L*a*b is announced in 1976 (SEII EM-MI 2002). It is mainly used in computer vision communities for image analysis and industrial applications. Nevertheless, it seems not of much interest by photogrammetrists.

The component L represents the light Lightness with value from 0 (black) to 100 (white) as defined below:

$$\begin{aligned} L &= 116 \cdot (Y/Wy)^{1/3} - 16 \quad \text{if } 0.008856 < (Y/Wy) \\ L &= 903.3 \cdot (Y/Wy) \qquad \text{else} \end{aligned} \tag{2}$$

Where (X, Y, Z) is the point to be converted, (Wx, Wy, Wz) the white point defined in CIE XYZ. The components *a* and *b* represent two differences defined below. In theory, component *a* varies from green (with value –120) to red (with value +120), component *b* varies from blue (with value –120) to yellow (with value +120).

$$\begin{aligned} a &= 500 \cdot (F(X/Wx) - F(Y/Wy)) \\ b &= 200 \cdot (F(Y/Wy) - F(Z/Wz)) \end{aligned} \tag{3}$$

Where (X, Y, Z) is the point to be converted, (Wx, Wy, Wz) the white point as defined in CIE XYZ. The point (X, Y, Z) can be obtained from equation (1) with RGB value of a pixel in the image. If $p > 0.008856$, then $F(p) = p^{1/3}$, otherwise $F(p) = 7.787 * p + 16/116$.

There is no direct relation between RGB and CIE L*a*b. The transformation from RGB to CIE L*a*b must be made indirectly through CIE XYZ. Firstly, RGB is transformed into CIE XYZ with equation (1), and then the received points into CIE L*a*b according to equation (2) and equation (3).

The component a of CIE L*a*b will be always negative for vegetations in standard RGB imagery and close to -120 for the strongest vegetative growth, while positive and close to +120 for the strongest vegetation in CIR imagery. That means no matter standard RGB or CIR image, CIE L*a*b is ready for image segmentation. Figure 4 (a) shows a standard RGB image acquired by digital camera in July 2004, Istanbul. There are trees, buildings, water and sky. Figure 4 (b) is the result of segmentation by CIE L*a*b. As can be seen, most trees are kept, while buildings, water and sky are successfully removed from the image, which verifies the feasibility of RGB image segmentation by CIE L*a*b.

Figure 4 (a)

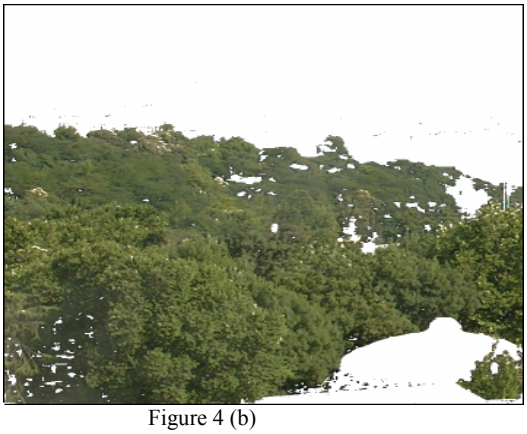

Figure 4 (b)

Figure 4. RGB Image and Result of Segmentation by CIE L*a*b

4. EXTRACTION OF TREE ROWS AND HEDGES

4.1 Image segmentation

Image segmentation by NDVI value for CIR images to extract vegetations is a well-known approach (Lyon 1998, Butenuth 2003). NDVI calculations are based on the principle that actively growing green plants strongly absorb radiation in the visible region of the spectrum such as Red region while strongly reflecting radiation in the Near Infrared region and thus a high NDVI value: NDVI = (NIR- Red)/(NIR + Red). Figure 5 shows the segmented CIR image of Figure 2 by NDVI information. In order to keep all potential tree rows and hedges, we adopt a relatively low threshold (NDVI = 0.1) in segmenting. White areas in the image are non-vegetation ones. As can be seen, results of segmentation in the upper left are not very satisfying, with some non-vegetation areas still remained.

The result of segmentation by CIE L*a*b with threshold a = 12 (equivalent to NDVI = 0.1) is shown in Figure 6. When compared with Figure 5, it can be seen that more non-vegetation regions are removed. Regions of tree rows and hedges are also clearer, and show very good line structures. So CIE L*a*b is used for image segmentation in this paper.

4.2 Line extraction and linking

Single tree and hedge are not of interest since they are nearly of no influence on soil protection. Tree rows or hedges usually appear line structures, or at least can be treated as combination of line segments. As can be seen from Figure 6, tree rows and hedges in the segmented image show very good line structures. Canny algorithm is used to extract these edges. Then the extracted edges are converted into longer line segments.

As shown in Figure 7, most borderline segments of tree rows and hedges have been extracted successfully. Lines of non-interested regions such as forests and urban can be masked out with the available GIS data, for example the center and lower-left part of Figure 7. Edges of field boundaries can be easily removed by CIE L*a*b information. But boundaries of grassland are difficult to remove because they also appear good line structure and positive a component of CIE L*a*b, for example the upper-right side of Figure 7. Another reason is that tree rows and hedges are sometimes connected to grassland (bottom of Figure 7). They have to be treated as potential tree rows and hedges at this step.

Afterwards, the remained line segments are linked in the along-line-direction by their inclination, direction and distances in between with perceptual grouping techniques. The linked lines will be longer than the initial ones and represent the borderlines of tree rows and hedges or grasslands (Figure 8).

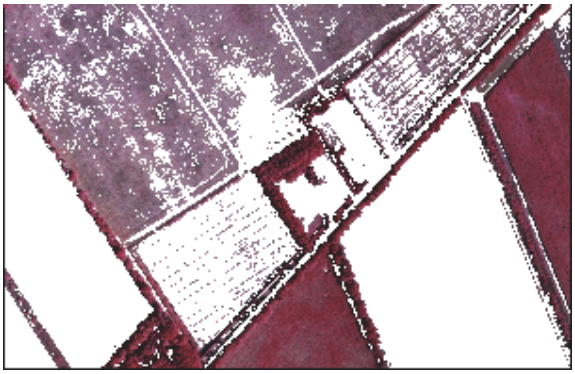

Figure 5. Result of Segmentation by NDVI

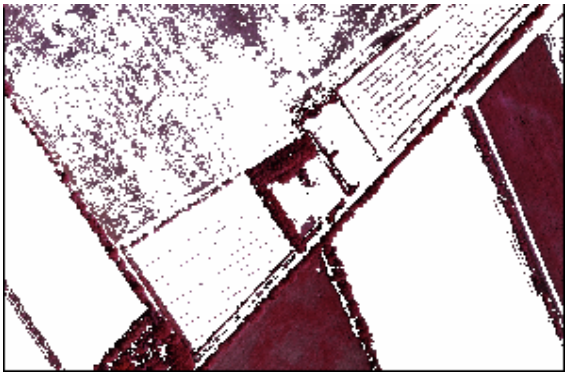

Figure 6. Result of Segmentation by CIE L*a*b

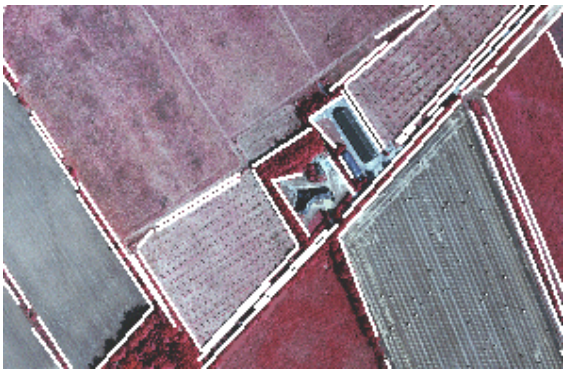

Figure 7. Extracted image lines

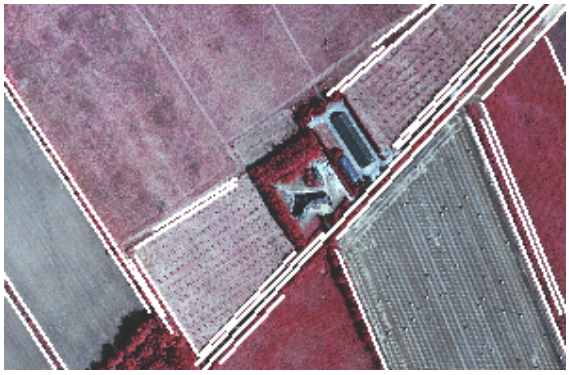

Figure 8. Linked line segments

4.3 Line grouping and matching

Tree rows and hedges always have two borders since they have a certain width. So the extracted lines of two borders (sometimes only borderline of one side can be extracted if the other side is connected to grassland or of low contrast in the image) should be grouped into one line segment. The line of the other side can be determined by a search algorithm within a certain distance in the cross-line-direction. DSM information is also considered during line grouping. The line pairs are combined together to get the centreline of tree row and hedge. As shown in Figure 9, all line pairs are combined together successfully.

If no corresponding line found, the line of interest will probably be the boundary of grassland and of course that of tree rows and hedges. For boundary of grassland, one side of it will be a region with low a value of CIE L*a*b while the other side a homogeneous region with high a value. This information is also helpful to remove borderlines of grassland. Usually, the grouped lines are not precisely the centerline of tree rows and hedges. Precise centerlines can be obtained by least squares image matching (Schenk 1999).

Figure 9. Grouped potential tree rows and hedges

4.4 Verifying with height information

After image segmentation, line extraction and grouping on both images of one stereo, the matched lines are the centerlines of tree rows and hedges. The conjugate lines on both images can be found with epipolar line and mean x-parallel of relative orientation because there are only a few candidates of the interested line. A global optimization is needed to make sure that no false corresponding exists.

The conjugate line pairs can be used to obtain the 3D lines in object space by forward intersection with known orientation parameters of the stereo images. As shown in Figure 10, lines without conjugates on the other image can be initially projected onto a level plane with mean height h_{start} of tree rows and hedges. The new height value $h(M_1)$ can be obtained from the DSM with the projected plane coordinate M_1. Then the image line can be projected onto level plane with the new height $h(M_1)$ to get new plane coordinates M_2. This recursive search procedure usually converges within a few iterations.

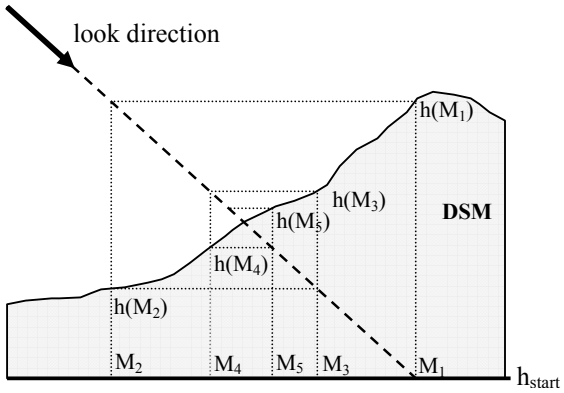

Figure 10. Height determination with single image and DSM

Figure 11. Results of extracted tree rows and hedges

The obtained 3D lines are potential tree rows and hedges. Roads, field boundaries, rivers and railways in GIS data are also potential search areas. All these information are compared with DSM to verify whether they are really tree rows and hedges. At this step, the remained boundaries of grassland can be easily removed because grassland will be usually wider than tree rows and hedges and thus a large area with same height information. Figure 11 shows the finally extracted tree rows and hedges.

5. EXPERIMENTAL RESULTS

In this section, the experimental results of the automatically extracted tree rows and hedges will be discussed. The testing area is located at an open landscape of Lower Saxony (Germany). GIS data, CIR stereo imagery with known camera orientations, and DSM are used as sources of information. Precision of the available GIS data is about 3m. CIR images are generated in early autumn when the tree rows and hedges are in an advanced period of growth. There are totally 132

CIR aerial images with 60% forward overlap and 60% side overlap. DSM of the test area is produced by VirtuoZo with ground control points measured from the GIS data.

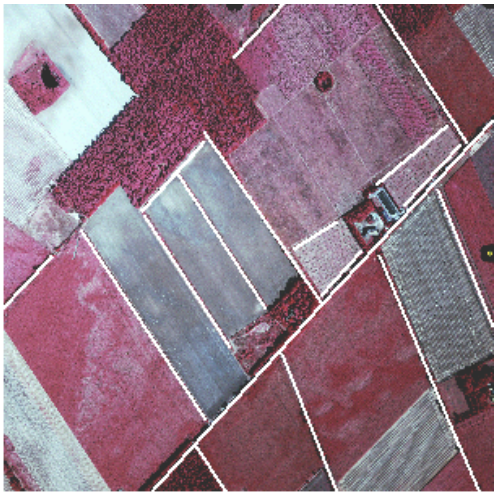

Figure 12 (a)

Figure 12 (b)

Figure 12. Final results of extracted tree rows and hedges

The general procedure of the proposed approach can be summarized as follows. Firstly, CIR image is segmented into vegetation and non-vegetation areas, and non-vegetation areas are removed from the image. Afterwards, lines are extracted from the segmented image, followed by removing of extracted lines that belong to non-interested regions such as forests and buildings according to the available GIS data. Then the remained lines are linked along-line-direction and then grouped cross-line-direction to get the centerline of tree rows and hedges. Finally, camera parameters, matched lines, DSM and GIS data are integrated to derive tree rows and hedges.

The extracted tree rows and hedges are described by their direct appearance in geometry, such as position, width and height. First results of extracted tree rows and hedges are quite satisfying. Figure 12 shows the extracted tree rows and hedges on a stereo pair. As can be seen, most tree rows and hedges are extracted automatically, only one hedge (center of figure 12a and center-left of figure 12b) is missing. When compared with lower left of Figure 8, one can see that the line of the missed hedge is extracted and linked successfully. This line is grouped into the adjacent longer line because they are very close to each other and the DSM information is not enough precise.

There already has the information of all tree rows and hedges obtained semi-automatically in the whole test area. When compared with these available reference data, the completeness and correctness of the extracted tree rows and hedges are both higher than 95%, which shows that the proposed approach works well in extraction of tree rows and hedges.

6. DISCUSSION

An effective approach of extraction tree rows and hedges by integrating GIS data, DSM and CIR aerial imagery is presented. Prior knowledge from GIS and DSM is essential to facilitate the extraction of interested objects. The extracted tree rows and hedges can be used in precision farming, soil monitoring and protection.

The proposed approach of image segmentation by CIE L*a*b has a well potential for extraction of vegetations from imagery because it always works no matter on standard RGB imagery or on CIR imagery. When compared with NDVI that only works on CIR imagery, CIE L*a*b is of great advantage for images already taken (for example, many years ago) with standard RGB format. Of course, synthetic evaluation of the ability of image segmentation with CIE L*a*b and NDVI needs further investigations.

Extraction of tree rows and hedges by integrating separately extracted field boundaries, orthoimage (if available) and the data already used in this paper will be our work in the near future. An overall evaluation of separately extracted tree rows and hedges and field boundaries to improve the completeness and correctness of the achieved results also need to be

performed.

ACKNOWLEDGEMENTS

The author would give many thanks to staffs of IPI, University of Hannover, especially Prof. Konecny, Prof. Heipke and Dr. Jacobsen for giving the opportunity to do this interesting work.

This work is also supported by National Natural Science Foundation of China (NSFC) with project number 40301041.

REFERENCES

1. E. P. Baltsavias, 2002. Object Extraction and Revision by Image Analysis Using Existing Geospatial Data and Knowledge: State-of-The-Art and Steps Towards Operational Systems. IAPRS, Vol. 34, Part 2: 13-22, Xi'an, China.
2. M. Butenuth, C. Heipke, 2003. Modelling the Integration of Heterogeneous Vector Data and Aerial Imagery. Proceedings ISPRS Workshop on Challenges in Geospatial Analysis, Integration and Visualization II, Stuttgart, Sept. 8-9.
3. M. Butenuth, 2004. Modelling the Extraction of Field Boundaries and Wind Erosion Obstacles from Aerial Imagery. International Archives of Photogrammetry and Remote Sensing, Vol.35 Part B4: 1065-1070.
4. P. Campadelli, R Schettini, S. Zuffi, 2000. A System for the Automatic Selection of Conspicuousness Color Sets for Qualitative Data Display and Visual Interface Design. Journal of Image and Graphics , Vol 5: 500-503.
5. M. G. Driehuyzen, 2003. Control of Wind Erosion. Ministry of Agriculture and Food, Government of British Columbia.
6. C. Heipke, K. Pakzad, B. M. Straub, 2000. Image Analysis for GIS Data Acquisition. Photogrammetric Record, Vol. 16: 963-985.
7. V. Lebrun, C. Toussaint, E. Pirard, 2000. On the Use of Image Analysis for Quantitative Monitoring of Stone Alteration. http://www.ulg.ac.be/mica/pdffiles/Marble_Color_Alteration.pdf
8. J. G. Lyon, D. Yuan, R. Lunetta, 1998. A Change Detection Experiment Using Vegetation Indices. Photogrammetric Engineering and Remote Sensing, Vol. 64: 143-150
9. SEII EM-MI 2002. Theory Perceive the Color, Introduction to Graphic of Computer. http://semmix.pl/color/default.htm.
10. B. M. Straub, 2003. Automatic Extraction of Trees from Aerial Images and Surface Models, ISPRS Conference on Photogrammetric Image Analysis, Munich, Germany
11. T. Schenk, 1999. Digital Photogrammetry. TerraScience, USA.
12. J. Wang, P. M. Rich, K. P. Price, et al, 2004. Relations between NDVI and Tree Productivity in the Central Great Plains. International Journal of Remote Sensing. Vol. 25: 3127-3138.
13. Y. J. Zhang, 2004. Extraction of Wind Erosion Obstacles by Integrating GIS-Data and Stereo Images. International Archives of Photogrammetry and Remote Sensing, Vol.35 Part B3: 375-380.